Published in final edited form as:
Science. 2009 October 30; 326(5953): 688–694. doi:10.1126/science.1179700.

The crystal structure of the ribosome bound to EF-Tu and aminoacyl-tRNA

T. Martin Schmeing, **Rebecca M. Voorhees**, **Ann C. Kelley**, **Yong-Gui Gao**, **Frank V. Murphy IV**[‡], **John R. Weir**[‡], and **V. Ramakrishnan**[†]
MRC Laboratory of Molecular Biology, Cambridge, UK, CB2 0QH

Abstract

The ribosome selects a correct tRNA for each amino acid added to the polypeptide chain, as directed by mRNA. Aminoacyl-tRNA is delivered to the ribosome by Elongation Factor-Tu (EF-Tu), which hydrolyzes GTP and releases tRNA in response to codon recognition. The signaling pathway that leads to GTP hydrolysis upon codon recognition is critical to accurate decoding. Here we present the crystal structure of the ribosome complexed with EF-Tu and aminoacyl-tRNA, refined to 3.6 Å resolution. The structure reveals details of the tRNA distortion that allows aminoacyl-tRNA to interact simultaneously with the decoding center of the 30S subunit and EF-Tu at the factor-binding site. A series of conformational changes in EF-Tu and aminoacyl-tRNA suggest a communication pathway between the decoding center and the GTPase center of EF-Tu.

Keywords

EF-Tu; 70S; ribosome; decoding; translation; aminoacyl-tRNA; tRNA delivery; protein synthesis; A/T; GTP; kirromycin

Introduction

The ribosome is the macromolecular enzyme that synthesizes proteins using aminoacyl-tRNA substrates as directed by an mRNA template. In order to faithfully translate the genetic information contained in mRNA, the ribosome must select cognate tRNA by its ability to base pair with the mRNA codon, a process termed decoding. EF-Tu, a translation factor with ribosome-dependent GTPase activity, delivers aminoacyl-tRNAs to the ribosome in a ternary complex (TC) of aminoacyl-tRNA•GTP•EF-Tu and plays an active role in ensuring the fidelity of decoding. Understanding the interplay between the TC and the ribosome that leads to the accurate translation of the mRNA message has been an active area of research for more than three decades.

Biochemical experiments have provided a wealth of information about the multi-step process of tRNA discrimination by the ribosome. Initial binding of TC occurs independently of mRNA (1), after which codon-anticodon pairs are sampled at the decoding center of the 30S subunit. Correct codon-anticodon matching induces conformational changes in three 16S nucleotides, A1492, A1493 and G530 (*E. coli* numbering, table s1), which monitor the geometry of the minor groove in the codon-anticodon helix (2) and accelerate the forward rate of selection (3). Binding of a near-cognate tRNA does not induce these changes (4),

[†]To whom correspondence should be addressed. ramak@mrc-lmb.cam.ac.uk.
[‡]Current Addresses: FVM: Northeastern Collaborative Access Team, Building 436, Argonne National Laboratory, Argonne, IL 60439, USA; JRW: Max-Planck-Institut für Biochemie, Abteilung Zelluläre Strukturbiologie, Am Klopferspitz 18, Martinsried D-82152 Germany

Europe PMC Funders Author Manuscripts

explaining why initial tRNA selection is more accurate than can be accounted for by the energetic differences between matched and mismatched anticodons alone (5). In addition to simple codon-anticodon base-pairing, physical properties of the tRNA body are also important for faithful decoding (6-11). Finally, the binding energy of a cognate tRNA is used to make an important “domain closure” of the 30S subunit (4), moving the “shoulder” domain closer to the TC (12).

The signal that codon recognition has occurred must then be transmitted to the GTPase center of EF-Tu. The ribosome could stimulate GTP hydrolysis using two strategies: first, by positioning catalytic residues in EF-Tu for GTP hydrolysis, and second by providing ribosomal components that function directly in catalysis. Domain 1 of EF-Tu is responsible for nucleotide binding, and rearrangements in this domain result in the opening of the “hydrophobic gate,” composed of residues Val20 in the P-loop and Ile60 in switch I, which prior to activation prevent access of the catalytic His84 to GTP(13). Mutation of His84 results in a 10^5 decrease in the rate of GTP hydrolysis by EF-Tu and this residue is thought to position and activate a water molecule to hydrolyze GTP (14). Ribosomal components implicated in GTPase activity include the Sarcin-Ricin loop (SRL) of 23S rRNA, located adjacent to the nucleotide binding pocket of EF-Tu (15); ribosomal protein L7/L12, which stimulates hydrolysis 2500-fold (16); and the L11 protein and proximal rRNA (17).

Hydrolysis of GTP and release of Pi by EF-Tu leads to lowered affinity for aminoacyl-tRNA and release from the ribosome. tRNA is then either accommodated into the peptidyl transferase center or rejected via a proofreading mechanism (18, 19). Proofreading and initial selection are separated by irreversible GTP hydrolysis, and their multiplicative effect accounts for the high accuracy of decoding (3, 20). Despite the wealth of biochemical data, the transmission of codon recognition to the GTPase center and the activation of GTP hydrolysis is not well understood.

Crystal structures of EF-Tu and TC have been determined for complexes with GDP and GTP analogues, as well as a variety of antibiotics ((13, 21, 22)(Protein Data Bank ID code 1OB2), and references therein). Isolated structures of EF-Tu revealed the global conformational change of domain 1 that occurs upon transition between the active (GTP) and inactive (GDP) states of the protein (13). The conformations of switch I and switch II, which form part of the GTPase center, also depend on the nucleotide state of EF-Tu. Notably, switch I became disordered in the complex of EF-Tu•GDP and the antibiotic methyl-kirromycin (21). TC structures reveal the substantial interaction surface between the tRNA and EF-Tu, including conserved interactions with A76 and the activated amino acid at the interface of domains 2 and 3 (22).

The complex of the TC stalled on the ribosome by the antibiotic kirromycin afforded the first visualization of EF-Tu delivering an aminoacyl-tRNA, by single particle cryo-electron microscopy (cryoEM) (23). The tRNA was distorted into what was called the “A/T” state (24) in order to interact simultaneously with the decoding center of the 30S subunit and EF-Tu, bound at the factor binding site in the intersubunit space (25),. Subsequent studies produced steady improvements, and the most recent reconstructions are to beyond 7 Å resolution (26, 27). These studies provided valuable information, but precise description of subtle conformational changes, the nature of the tRNA distortion, and atomic interactions, along with the mechanistic insights to which they lead, all require higher resolution structures.

EF-Tu•tRNA bound to the ribosome

Here we present the crystal structure of the 70S ribosome from *Thermus thermophilus* in complex with $tRNA^{Phe}$ in the E and P sites, mRNA, and the ternary complex (TC) of EF-

Tu•Thr-tRNA^{Thr}•GDP, stabilized by the antibiotics kirromycin and paromomycin, refined to 3.6 Å resolution (I/σ=2 at 3.75 Å) (Table s1, Fig. 1). Kirromycin prevents rearrangements of EF-Tu following GTP hydrolysis and Pi release, thus trapping the complex on the ribosome(28). The domain conformation of EF-Tu in this state is thought to be similar to that at the GTP transition state (29). EF-Tu and Thr-tRNA^{Thr} have been built into electron density, with many side chains of EF-Tu, bases of tRNA, both antibiotics and GDP clearly resolved (Fig. 1a). As expected, the ribosome is in a non-ratcheted state with P- and E-site tRNAs in the classic states, and a similar overall conformation to the structure containing an accommodated aminoacyl-tRNA (30) (Fig. 1b). The largest conformational changes of the ribosome are in the L1 rRNA region and helices 43-44 of the 23S rRNA, which includes the L11 binding site and becomes more ordered to interact with the elbow of the tRNA (Fig. 1c). The aminoacyl-tRNA is bound in the A/T state, and conformational changes in the 30S subunit indicative of cognate tRNA binding are observed including the flipping out of bases G530, A1492 and A1493 of the 16S rRNA and the “closing” of the 30S subunit (2). EF-Tu interacts with the factor binding site and the 30S shoulder. This overall conformation is in good agreement with previous lower-resolution cryo-EM studies (24, 26, 27).

Distortion of tRNA

In order to adopt the A/T conformation, the aminoacyl-tRNA must be distorted substantially to allow the ~30° bend required to simultaneously bind the mRNA codon and EF-Tu. There are two distinct areas of distortion in the tRNA body: a bend in a 13 nucleotide region of the anticodon stem, and a change in the positioning of the D-stem with respect to the acceptor and T-stem contiguous stack. The very 3′ end of the tRNA is also distorted, as the backbone of residues 72-75 has shifted by up to 6 Å and nucleotides C72 and C75 have swung outward. While this conformation has a significant mechanistic role (described below), it is not directly connected to the bent conformation of the tRNA body. Notably, the acceptor helix and anticodon adopt the canonical conformation, and the ASL of the A/T tRNA interacts with the decoding center in the same way as fully accommodated cognate A-site tRNA (A/A tRNA) (30) (Fig. 2a).

The anticodon stem distortion involves a reduction of helical twist and a widening of the phosphate backbone. The distortion begins at base pair 30:40, where the tRNA adopts a smooth bend involving nucleotides 25-30 and 40-48, rather then a kink as previously proposed (24). The helix in this region becomes under-twisted by up to 14°, from base pairs 30:40 through 25:45, to facilitate this bend (Fig. 2b). The distortion also includes a widening of the strands directly above the anticodon stem, as the phosphate-phosphate distance of nucleotides 25-45 and 26-44 are approximately 2 and 1 Å wider than in canonical tRNA. The observed widening explains the biochemical result that mutation of the 27:43 base pair gives an error-prone phenotype (9); weakening of this base pair could decrease the energy required to separate the strands at the adjacent nucleotides, allowing the distortion to occur more easily and thus the binding of mismatched tRNA. Indeed, the 27:43 base pair appears to be disrupted in the structure of the A/T tRNA, though the electron density for the base of C27 is not well defined.

Ribosome binding also causes a second region of distortion, which moves the D-stem away from the T and acceptor stem stack (Fig. 2c). This movement does not affect the canonical stack between the T and acceptor stems, which superimpose very well between the isolated and ribosomal-bound TCs (P-P r.m.s.d of 1.3 Å). The distortion of the A/T tRNA compared to that of isolated TC begins at the junction of the acceptor stem and D-stem, around unpaired nucleotides 8-9, which results in a ~5 Å swing of the D arm. This rearrangement separates the 15:48 and 16:59 base pairs, but the displacement is smaller at the distal bases of the D-loop (~G19), and the elbow interactions are largely unaltered.

That codon recognition involves a tRNA distortion with a rearrangement of the D-stem explains several experimental observations (Fig. 2d). A proflavin moiety, inserted at position 16 or 17, produces a fluorescent signal upon codon recognition (1), which is easily explained by the ~5 Å displacement of these nucleotides in the distorted A/T tRNA. The Hirsh suppressor tRNA is a $tRNA^{Trp}$ with a G24A mutation that allows Trp incorporation at UGA stop codons (6) G24 is normally base paired to C11, but in the distorted conformation the tRNA backbone across these nucleotides is ~1 Å farther apart than in a canonical tRNA, suggesting how the Hirsh suppressor can more easily sample the distorted conformation (7, 8). Indeed, a chemical crosslink between D-stem nucleotide 13 and nucleotide 8, which is directly adjacent to the acceptor stem, occurs less frequently in the Hirsh tRNA background (31); these nucleotides separate in the distorted conformation. Conversely, the 8-13 crosslink would reduce the propensity for adopting the distortion required for decoding, and has been show to limit the miscoding activity of the Hirsh suppressor tRNAs (10). The disruption of the 9:12:23 triple also gives a phenotype similar to the Hirsh suppressor (8). Interruption of this stabilizing interaction would facilitate deformation of the tRNA in the D-stem region. However, as the triple is intact in the A/T state, mutation of this base triple would likely allow formation of an altered distortion that achieves a similar bend to that observed for a wild-type tRNA. These mutations within the tRNA body would reduce the energetic penalty for distortion, which is normally precisely balanced against the energy derived from cognate codon-anticodon interaction. Thus productive binding of TC and GTP hydrolysis can occur in these cases for even a near-cognate codon-anticodon interaction, as the energetic barrier for adopting the A/T conformation has been reduced.

Although the proposed nature of the tRNA distortion differed in older cryo-EM studies, its general description in the most recent cryo-EM work is similar to that observed in the present X-ray crystal structure (26, 27). While a distortion of the anticodon stem was observed, the widening of the tRNA above the anticodon stem was not detected and the extent of the D-stem movement is significantly larger then reported.

Ribosomal stabilization of distorted tRNA: few but important interactions

The highly distorted tRNA must be stabilized by interactions with the ribosome and EF-Tu. The structure reveals that the A/T tRNA interacts primarily with the decoding center and EF-Tu while forming very few additional contacts with the ribosome (Fig. 1c). The decoding center interacts with the tRNA in a near identical manner to accommodated tRNA (30). A single additional sugar packing interaction between residue C25 of the tRNA and C1914 of 23S rRNA helix 69 is observed in this region.

In addition to the decoding center, the tRNA interacts with three regions of the ribosome: the shoulder domain of the 16S rRNA, ribosomal protein S12, and the L11 region of 23S rRNA (Fig. 1c). Distortion in the 3′ end of the A/T tRNA between residues 72-75 allows C75 to pack between EF-Tu residue 219 and the flipped base of A55, a residue which is 99.5% conserved in all species of known sequence (Fig. 3). Although A55 changes conformation, the rest of helix 5 of 16S rRNA is largely unaltered. S12 contacts the tRNA at the acceptor arm/D stem junction. In this region, the side chain of Gln74 is within hydrogen bonding distance of the 2′OH of A67 and the side chain of His76 interacts with the sugar of residue U68. These two S12 residues form part of the highly conserved QEH sequence. Mutation of His76 leads to streptomycin-resistance, suggesting that this contact is important for proper TC binding (32). The S12 interactions were previously reported to be with tRNA residue 69 (26). In addition, EF-Tu contacts S12 with a single salt-bridge between Glu249 of domain 2 of EF-Tu and Lys119 of S12.

The L11 rRNA interacts with the tRNA elbow at residue dihydroU20 which is within hydrogen bonding distance of U1068, and C56 through a packing interaction with A1067. The latter interaction is consistent with biochemical data showing that mutation of A1067U resulted in a 3-fold decrease in the rate of ternary complex binding to the ribosome and a 2-fold decrease in the rate of GTP-hydrolysis for cognate tRNA(33).

Considering only these few interactions outside the decoding center, the surface area of the A/T tRNA buried by the ribosome is only 482 $Å^2$. Indeed the most extensive interactions of tRNA are those with EF-Tu, which bury 1540 $Å^2$ of surface area. The movement of the strained tRNA into the peptidyl transferase center upon release of EF-Tu would require disruption of only a few interactions with the ribosome, an energetic barrier that should be easily surmountable by the potential energy stored in the strained tRNA.

An important interaction between domain 2 and the 16S rRNA

The overall domain orientation of the ribosome-bound EF-Tu is very similar to that of the isolated methyl-kirromycin structure (21, 27), however a small concerted conformational change is observed in surface residues of domain 2 (Fig. 3a). While those residues forming the interface between domains 2 and 3 remain unaltered, domain 2 residues 256-273 and 219-226, the latter comprising a β-turn near the 3′ end of the A/T tRNA, shift to allow two loops of EF-Tu to contact the 16S rRNA shoulder (Fig. 3a/b). These interactions are facilitated by the domain closure of the 30S subunit, which moves the 16S rRNA towards EF-Tu. As these movements are not observed in the isolated structures of EF-Tu, even when similarly bound to both GDP and kirromycin, they are presumably a result of ribosome binding. Residues 278-281 interact with 16S rRNA 367-368 via packing, in addition to hydrogen bonding between Arg279 and U368. The second of these loops of EF-Tu packs into a pocket of 16S rRNA made by residues 55-56, 357-358 and 368. Hydrophobic interactions include that between Thr221 and 16S residues A55 and U56, and between Gly222 and U368, while hydrogen bonding interactions occur between Arg223 and Gly222 and U368 and G357, respectively. This loop undergoes the most marked change upon ribosome binding and the contacts may be of particular importance, as 4 of the 7 residues between 219-226 are over 99% conserved in all species, including humans. Furthermore, hydrogen-bonding interactions with both loops of EF-Tu occur with residue U368, which is 99.7% conserved across all species.

Mutational and biochemical data highlight the importance of the interaction between domain 2 of EF-Tu and the shoulder of the 30S subunit. Mutation of Gly222 to an aspartate prevents hydrolysis of GTP by EF-Tu, and thus protein synthesis, at physiological Mg^{2+} concentrations (34, 35). At Mg^{2+} concentrations above 10 mM the G222D mutant EF-Tu can hydrolyze GTP and allow tRNA accommodation, although via a somewhat altered pathway (34). Further, kinetic data suggested that the G222D mutant EF-Tu was specifically deficient in its ability to transmit codon-anticodon recognition to the GTPase center perhaps by preventing a conformational change in EF-Tu (34). Replacement of the highly conserved Gly222 would likely prevent the conformational change in this loop required for interaction with the 16S rRNA. Additionally, placing a large negatively charged aspartate in a position that abuts the phosphate backbone of the 16S rRNA would be electrostatically unfavorable. However at Mg^{2+} concentrations above 10 mM this negative charge is likely screened by the divalent cations, partially rescuing the deficiency of the G222D mutant EF-Tu.

Shoulder binding alters certain interactions of EF-Tu with tRNA

Upon ribosome binding, local conformational changes of EF-Tu in both domain 2 and switch II alter the nature of a specific subset of the contacts between EF-Tu and the tRNA (Fig. 3c). Despite the suggestion from a cryo-EM study (26), the contacts between EF-Tu

and the aminoacyl-tRNA are similar to those observed in the isolated structure of TC for much of the binding surface, including those involving the tRNA T-stem and parts of the acceptor stem (22). Likewise, interactions with the activated amino acid of aminoacyl-tRNA are maintained, including a hydrogen bond between Arg262 and the backbone carbonyl and Asn273 with the primary amine, as well as several hydrogen bonds with A76.

In solution, EF-Tu protects the labile ester bond of aminoacyl-tRNA, and must continue to prevent hydrolysis of this bond upon binding to the ribosome. Maintaining these interactions with the amino acid while also allowing the conformational change of domain 2 towards the 16S rRNA may in part require the observed distortion of the 3′ end of the A/T tRNA (Fig. 3), and the novel EF-Tu – tRNA interactions. This distortion of the tRNA between residues 72-75 moves the bases of C74 and C75 to interact with Arg283 and Thr219-Ile220 respectively (fig. s1), and shifts the tRNA backbone 5-6 Å away from the position of switch I in the isolated GDPNP:ternary complex (Fig. 3d) (22). This would disrupt the interaction of tRNA residues 73-74 with switch I, perhaps leading to the disordering of switch I, for which we see no electron density.

Ribosome binding shifts the switch II loop towards the backbone of the tRNA (this motion is also mimicked by binding of kirromycin (Protein Data Bank ID code 1OB2)), allowing interaction between the phosphate oxygen of C65 with the side chain of Lys89. In a recent cryo-EM study however, the authors suggested, based on a comparison with the isolated kirromycin-TC structure, that upon ribosome binding the acceptor arm of the tRNA shifted closer to switch II of EF-Tu, facilitating formation of an interaction between the conserved Asp86 and the tRNA (26). However, a negatively charged Asp side chain would interact with the phosphate backbone in a repulsive manner. We find the acceptor arm of the tRNA not to be distorted from the canonical structure, evidenced by the superimposition of this region with that from the isolated TC (22) (Fig. 3c). With this comparison, it is instead a local movement of the switch II loop (including Asp86) that allows the altered interaction of switch II with the acceptor stem.

GTPase activation by the ribosome

Switch I and II, along with the P loop are functional components of the GTPase center of EF-Tu. GTP is likely protected from hydrolysis by a “hydrophobic gate” of Ile60 (switch I) and Val20 (P loop) (13). During ribosome-induced GTP hydrolysis this gate is opened, allowing putative catalytic residues Gly83 and His84 of switch II to interact with the γ-phosphate or nucleophilic water (13, 14). In the present structure the catalytic His84 is positioned away from the G-nucleotide in its inactivated position (22), consistent with the post-GTPase state of this complex (fig. s2). The switch II loop and the P-loop are well ordered, but no density is observed for the switch I region from residues 42-65 including Ile60 of the hydrophobic gate. This disordering of switch I may be the mechanism of opening the hydrophobic gate, as observed in the isolated structure of EF-Tu in complex with GDP and methyl-kirromycin (21).

The disorder of switch I seen here is in contrast to the recent cryo-EM structure of the ribosome bound to the ternary complex in the same state(26) that reports weak density for an alternate conformation of switch I interacting with h8 and h14 of the 16S rRNA. There is no evidence for this conformation in the current study, even in electron density maps calculated to low-resolution and displayed at low threshold, consistent with another cryo-EM structure (27).

Perhaps because the reported structure does not depict the transition state of the GTP hydrolysis reaction, we cannot identify ribosomal components that could directly function in catalysis, despite the proposal that additional catalytic groups may be involved (36). No

density was observed for ribosomal protein L7/L12 which is known to be important for stimulating GTP hydrolysis by the ribosome, although perhaps through indirect action (16). Also important for GTP hydrolysis is the SRL of the 23S rRNA, which interacts with domain 1 of EF-Tu. No conformational changes of the SRL are observed when compared to that containing an anticodon stem loop in the A site(37). However, the catalytic His84 interacts with the 2′OH of G2661, likely holding the residue in its inactivated state. (fig. s2). Additionally, EF-Tu residue His19 is within hydrogen bonding distance of a phosphate oxygen of G2661 of the SRL. Mutation of SRL residue G2661C results in hyperaccurate ribosomes, perhaps by disrupting an interaction between EF-Tu and the SRL, further destabilizing the binding of near-cognate tRNA (38). Though Val20 (P-loop), one part of the hydrophobic gate, is positioned close to these interactions, the SRL does not seem to be directly involved in opening the hydrophobic gate. Furthermore, the closest nucleotide of the SRL is ~5.5 Å from the GDP sugar, which would be too far to be directly involved in stimulating GTP hydrolysis.

Insights into the Decoding Pathway

The crystal structure of EF-Tu trapped on the ribosome provides an opportunity to analyze the complete decoding pathway in its structural context and to propose the mechanism by which codon-anticodon recognition is communicated to the GTPase center over 80 Å away (Fig 4).

Initial binding and sampling

The multimeric L7/L12 recruits TC for initial reversible and mRNA-independent binding (Fig. 4a) (1, 39). In the initial TC conformation, the position of the tRNA allows sampling of codon – anticodon matches without excessive tRNA strain (Fig. 4b, s3)(34).

Codon recognition and GTPase Activation

The aminoacyl-tRNA samples a strained conformation until codon-anticodon recognition takes place (40), which results in the 30S subunit domain closure (Fig. 4c)(2). The precisely-tuned flexibility of the tRNA facilitates its distortion (11). EF-Tu is pulled into its productive conformation by interactions with the distorted tRNA and by contacts with the ribosome.

Binding of EF-Tu induces a shift of regions of domain 2—including the β-turn comprised of residues 219-226—towards the now “closed” 16S rRNA. This leads to a ~5 Å distortion of the 3′ end of the tRNA (residues 72-75), which disrupts interactions between the tRNA and switch I loop. Loss of these stabilizing interactions leads to disordering of switch I, which opens the hydrophobic gate, thereby transmitting the signal that codon recognition has taken place to the heart of the GTPase center. This proposal explains why cleavage of switch I between residues Arg57 and Gly58 or Lys51 and Ala52 causes defects in ribosome-induced GTP hydrolysis by EF-Tu (41), as these cleavages would prevent transmission of the signal from the 3′ end of the tRNA to the GTPase center.

Opening of the hydrophobic gate allows putative catalytic residues Gly83 and His84 of switch II to interact with the γ-phosphate and/or activate a water molecule, triggering GTP hydrolysis (13, 14, 42).

Nucleotide Induced Conformation Change of EF-Tu

Following GTP hydrolysis and Pi release, EF-Tu undergoes a conformational change to its GDP form, which involves a ~100° swing of the G-domain relative to domains 2 and 3 (Fig. 4d) (13). This movement would disrupt the interactions of the G-domain with the SRL, as

well as those between switch II and the tRNA acceptor arm, separating TC and leading to dissociation of EF-Tu from the ribosome.

Accommodation and Proofreading

In the absence of EF-Tu, the few interactions between the distorted tRNA and the ribosome leave a largely clear path to the PTC (Fig. 1c, 4e). The energetics of accommodation must be finely balanced, as near-cognate tRNAs are discriminated against at this second checkpoint in decoding (3). A near-cognate tRNA would likely have weaker interactions with the decoding center, as it cannot induce the closed 30S conformation, characteristic of cognate tRNA binding (4). Therefore, as the tRNA reverts to its relaxed form, near-cognate tRNA might more easily disengage from the decoding center rather then swing into the PTC, providing the molecular mechanism for proofreading (4, 43). Once accommodation is complete, peptide bond formation is very rapid and the proper incoming amino acid is added to the nascent peptide chain, thus achieving the goal of decoding.

Supplementary Material

Refer to Web version on PubMed Central for supplementary material.

Acknowledgments

We thank M. Madan Babu and Peter Lukowski for help with data analysis, Gordon Leonard and Sandor Brockhauser for their guidance and advice with data collection at the European Synchrotron Light Source beamline ID14.4, Clemens Schultze-Briese and Anuschka Pauluhn for help with initial diffraction studies performed at the Swiss Light Source, and Larissa Ulisko for preparation of additional images. This work was supported by the Medical Research Council UK, the Wellcome Trust, the Agouron Institute and the Louis-Jeantet Foundation. RV is the recipient of a Gates-Cambridge scholarship. TMS received support from the Human Frontiers Science Program Organization, and Emmanuel College, University of Cambridge. The structure has been deposited at the Protein Data Bank with accession codes 2WRN, 2WRO, 2WRQ, and 2WRR.

References

1. Rodnina MV, Pape T, Fricke R, Kuhn L, Wintermeyer W. J Biol Chem. 1996; 271:646. [PubMed: 8557669]
2. Ogle JM, et al. Science. 2001; 292:897. [PubMed: 11340196]
3. Gromadski KB, Rodnina MV. Mol Cell. 2004; 13:191. [PubMed: 14759365]
4. Ogle JM, Murphy FV, Tarry MJ, Ramakrishnan V. Cell. 2002; 111:721. [PubMed: 12464183]
5. Xia T, et al. Biochemistry. 1998; 37:14719. [PubMed: 9778347]
6. Hirsh D. Nature. 1970; 228:57. [PubMed: 4917265]
7. Cochella L, Green R. Science. 2005; 308:1178. [PubMed: 15905403]
8. Smith D, Yarus M. J Mol Biol. 1989; 206:503. [PubMed: 2469804]
9. Schultz DW, Yarus M. J Mol Biol. 1994; 235:1381. [PubMed: 8107080]
10. Vacher J, Buckingham RH. J Mol Biol. 1979; 129:287. [PubMed: 383994]
11. Piepenburg O, et al. Biochemistry. 2000; 39:1734. [PubMed: 10677222]
12. Ogle JM, Ramakrishnan V. Ann Rev Biochem. 2005; 74:129. [PubMed: 15952884]
13. Berchtold H, et al. Nature. 1993; 365:126. [PubMed: 8371755]
14. Daviter T, Wieden HJ, Rodnina MV. J Mol Biol. 2003; 332:689. [PubMed: 12963376]
15. Moazed D, Robertson JM, Noller HF. Nature. 1988; 334:362. [PubMed: 2455872]
16. Mohr D, Wintermeyer W, Rodnina MV. Biochemistry. 2002; 41:12520. [PubMed: 12369843]
17. Bourne HR, Sanders DA, McCormick F. Nature. 1991; 349:117. [PubMed: 1898771]
18. Thompson RC, Stone PJ. Proc Natl Acad Sci. 1977; 74:198. [PubMed: 319457]
19. Ruusala T, Ehrenberg M, Kurland CG. Embo J. 1982; 1:741. [PubMed: 6765234]

20. Blanchard SC, Gonzalez RL, Kim HD, Chu S, Puglisi JD. Nat Struct Mol Biol. 2004; 11:1008. [PubMed: 15448679]
21. Vogeley L, Palm GJ, Mesters JR, Hilgenfeld R. J Biol Chem. 2001; 276:17149. [PubMed: 11278992]
22. Nissen P, et al. Science. 1995; 270:1464. [PubMed: 7491491]
23. Stark H, et al. Nature. 1997; 389:403. [PubMed: 9311785]
24. Valle M, et al. Embo J. 2002; 21:3557. [PubMed: 12093756]
25. Moazed D, Noller HF. Cell. 1989; 57:585. [PubMed: 2470511]
26. Villa E, et al. Proc Natl Acad Sci U S A. 2009; 106:1063. [PubMed: 19122150]
27. Schuette JC, et al. Embo J. 2009; 28:755. [PubMed: 19229291]
28. Kothe U, Rodnina MV. Biochemistry. 2006; 45:12767. [PubMed: 17042495]
29. Rodnina MV, Fricke R, Wintermeyer W. Biochemistry. 1994; 33:12267. [PubMed: 7918447]
30. Voorhees RM, Weixlbaumer A, Loakes D, Kelley AC, Ramakrishnan V. Nat Struct Mol Biol. 2009
31. Favre A, Buchingham R, Thomas G. Nucleic Acids Res. 1975; 2:1421. [PubMed: 1101224]
32. Gregory ST, Carr JF, Dahlberg AE. RNA. 2009; 15:208. [PubMed: 19095621]
33. Saarma U, Remme J, Ehrenberg M, Bilgin N. J Mol Biol. 1997; 272:327. [PubMed: 9325093]
34. Vorstenbosch E, Pape T, Rodnina MV, Kraal B, Wintermeyer W. Embo J. 1996; 15:6766. [PubMed: 8978702]
35. Swart GW, Parmeggiani A, Kraal B, Bosch L. Biochemistry. 1987; 26:2047. [PubMed: 3297141]
36. Rodnina MV. Proc Natl Acad Sci U S A. 2009; 106:969. [PubMed: 19164543]
37. Selmer M, et al. Science. 2006; 313:1935. [PubMed: 16959973]
38. Bilgin N, Ehrenberg M. J Mol Biol. 1994; 235:813. [PubMed: 7507174]
39. Diaconu M, et al. Cell. 2005; 121:991. [PubMed: 15989950]
40. Lee TH, Blanchard SC, Kim HD, Puglisi JD, Chu S. Proc Natl Acad Sci U S A. 2007; 104:13661. [PubMed: 17699629]
41. Zeidler W, et al. Eur J Biochem. 1996; 239:265. [PubMed: 8706729]
42. Knudsen C, Wieden HJ, Rodnina MV. J Biol Chem. 2001; 276:22183. [PubMed: 11304547]
43. Pape T, Wintermeyer W, Rodnina M. Embo J. 1999; 18:3800. [PubMed: 10393195]

Europe PMC Funders Author Manuscripts

Europe PMC Funders Author Manuscripts

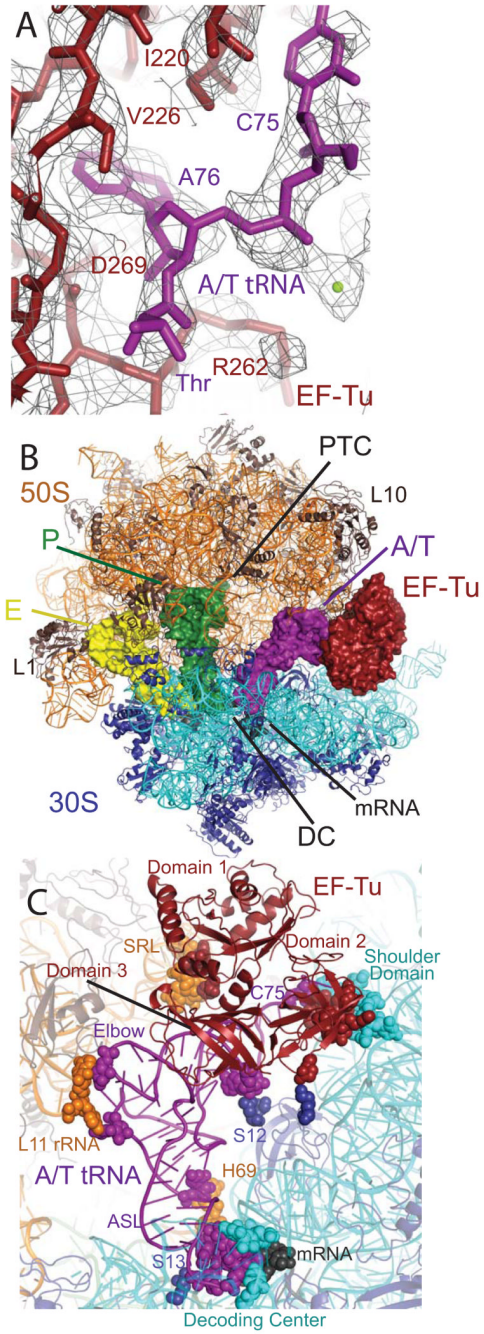

Fig. 1.

Structure of EF-Tu and aminoacyl-tRNA bound to the ribosome. **(A)** Representative electron density from an unbiased F_o - F_c map, displayed at 1.3σ, with the refined model of EF-Tu (red) and Thr-tRNA^{Thr} (purple). **(B)** Overall view of the complex, with EF-Tu and tRNAs depicted as surfaces, and rRNA and protein as cartoons. **(C)** Contacts between TC and the ribosome, with interacting residues shown as spheres.

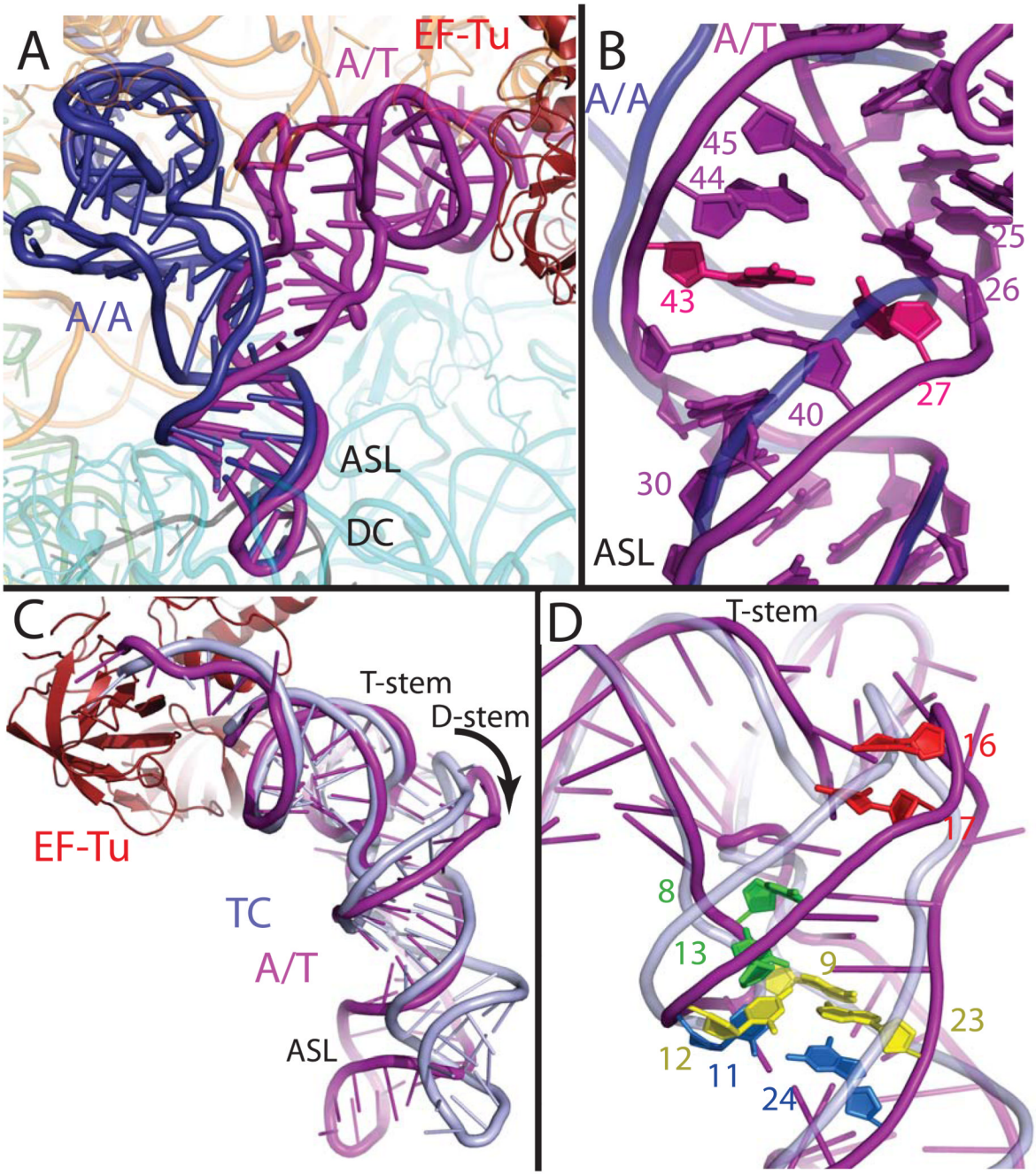

Fig. 2.

Distortion of aminoacyl-tRNA in the A/T state. **(A)** Comparison of the A/T tRNA (purple) with the fully accommodated canonical A/A tRNA (dark blue) (30) shows the overall extent of the tRNA disortion. **(B)** The structures diverge in the anticodon stem loop (ASL) with a reduction of helical twist after basepair 30:40, and separation of the phosphate-sugar backbones at nucleotides 25-45 and 26-44. Disruption of the 27:43 base pair (pink) (9) would facilitate this strand separation. **(C)** Comparison of the A/T tRNA with tRNA of the isolated TC (light blue) (22) highlights the swinging out and ~5Å shift of D-arm nucleotides. **(D)** The distortion rationalizes data pertaining to proflavin insertions at nucleotides 16-17

(bright red) (1), cross-linking of nucleotides 8 and 13 (green) (31), and mutations of the Hirsh base pair 24:11 (aqua) (6, 8) and 9:12:23 triple (yellow) (8).

Europe PMC Funders Author Manuscripts

Europe PMC Funders Author Manuscripts

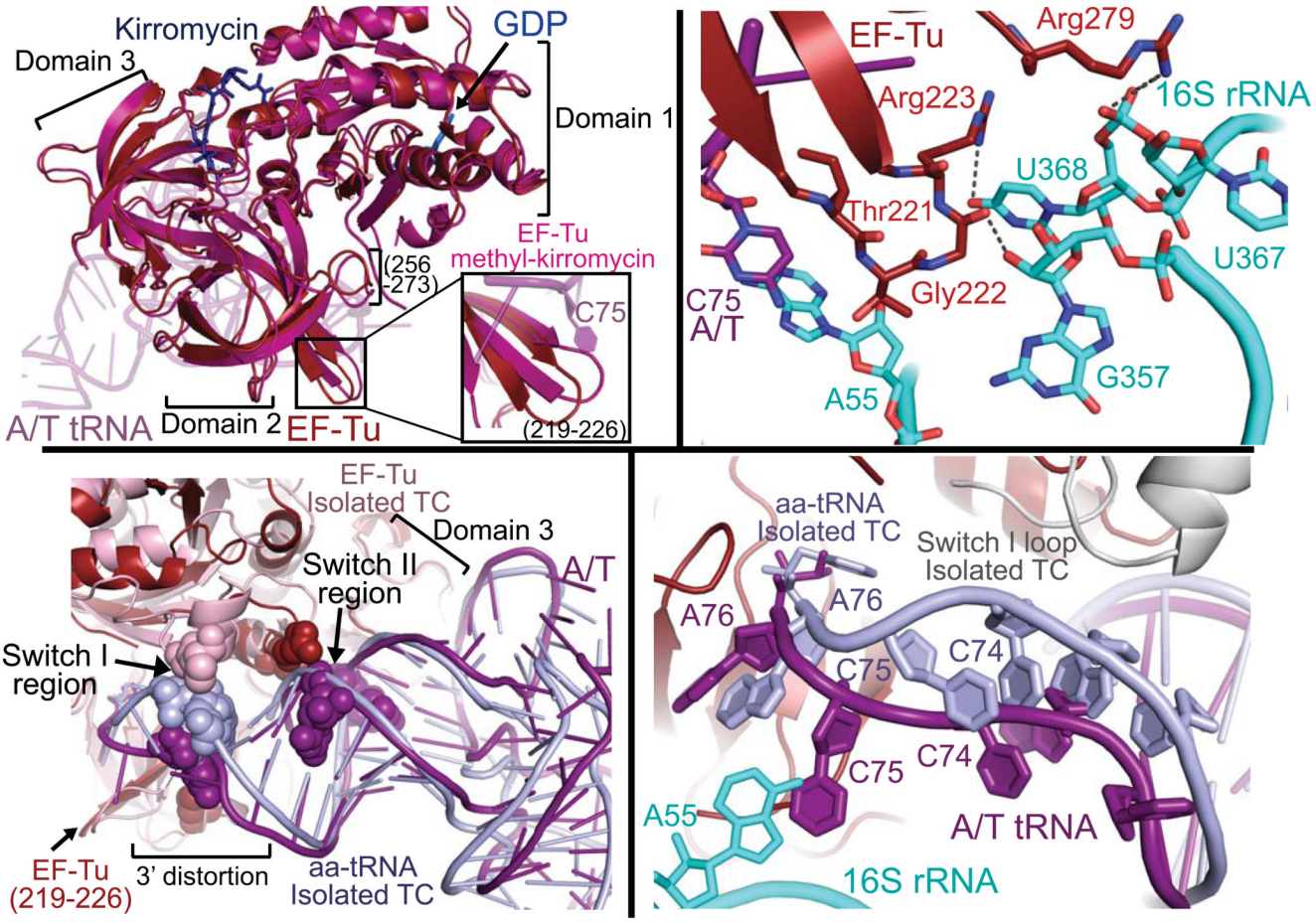

Fig. 3.

Changes of EF-Tu upon ribosome binding. **(A)** EF-Tu bound to the ribosome (red) adopts a similar conformation to the isolated EF-Tu methyl-kirromycin complex (hot pink)(21), but ribosome binding induces a shift in domain 2 loops including residues 256-273 and 219-226 (inset). **(B)** The detailed interactions between EF-Tu domain 2 and the shoulder domain of 16S rRNA (cyan). **(C)** Ribosome binding alters some of the contacts between EF-Tu and tRNA. Interaction of domain 3 with the T-stem is largely unchanged when compared to the isolated TC (22) but that of switch II with the 5′ end of tRNA is altered, and the switch I contact with the 3′ end is abolished. **(D)** Interaction with the 30S shoulder distorts the 3′ end of tRNA, separating it from switch I, which becomes disordered. The ordered switch I from the isolated TC (grey) is shown as comparison.

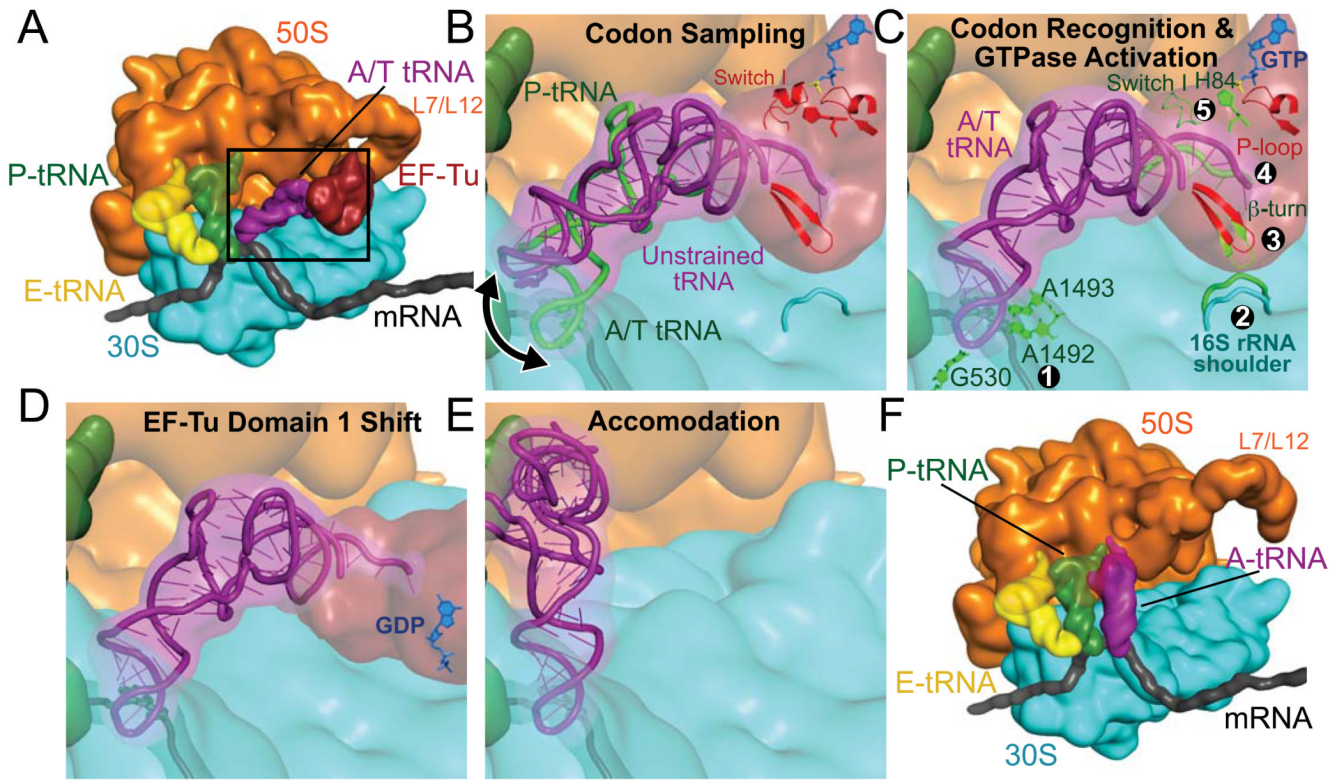

Fig. 4.

Schematic representation of the decoding pathway. **(A)** The L7/L12 stalk recruits TC to a ribosome with deacylated tRNA in the E site and peptidyl-tRNA in the P site. The black frame represents the enlarged area in panels (B)-(E). **(B)** The tRNA samples codon:anticodon pairing until a match **(C)** is sensed, by decoding center nucleotides 530 and 1492-3 ①. Codon recognition triggers domain closure of the 30S subunit ②, bringing the shoulder domain into contact with EF-Tu, and shifting the β-loop at 230-237 of domain 2 ③. This changes the conformation of the acceptor end of tRNA ④, disrupting its contacts with switch I, which becomes disordered ⑤, opening the hydrophobic gate to allow His84 to catalyze GTP hydrolysis. **(D)** GTP hydrolysis and P_i release cause domain rearrangement of EF-Tu, leading to its release from the ribosome and **(E-F)** accommodation of aminoacyl-tRNA.

Europe PMC Funders Author Manuscripts